Open Access Online Journal on Astronomy and Astrophysics

Acta Astrophysica Taurica

www.astrophysicatauricum.org

Acta Astrophys. Tau. 6(1), 5–8 (2025)

Ultraviolet emission of unipolar active regions and a relation between its intensity and magnetic flux decay rate

A. Plotnikov

Crimean Astrophysical Observatory, Nauchny 298409
e-mail: plotnikov.andrey.alex@yandex.ru

Received 23 July 2024

ABSTRACT

This study uses data on 617 active regions (ARs) acquired by the Solar Dynamics Observatory. Unipolar ARs exhibit a lower density of He II 304 Å ultraviolet (UV) emission above sunspots as compared to the ARs of other types. Bipolar and multipolar ARs, regardless of their magnetic flux, show a similar density of UV emission above sunspots. In contrast, in unipolar ARs, the UV emission density increases with increasing magnetic flux. This relationship can be used to estimate the magnetic flux values from the maps of UV emission density. Additionally, the total unsigned magnetic flux decay rate is in moderate correlation with the UV emission above sunspots. This correlation may help to explain the phenomenon of slow-decaying unipolar ARs.

Key words: Sun, active regions, magnetic flux decay, transition layer

1 Introduction

The power-law dependence between the the magnetic flux decay rate in an active region (AR) and the maximum value of the magnetic flux in it was shown in Plotnikov et al. (2023). Moreover, the authors detected a cluster of unipolar ARs exhibiting a significantly lower decay rate than it would follow from the power law (based on the magnitude of the magnetic flux in these ARs). It is worth noting that the unipolar AR is understood as an AR with no sunspots and pores visible in white light in its trailing polarity.

Due to the fact that the beginning of the decay process for such ARs is not observed (an AR comes out from behind the limb already in the decay phase), it is of interest to study their behavior behind the solar limb.

For these purposes, it is possible to use data from space observatories capable of observing the Sun from the angles significantly different from the Earth's one. The Solar Orbiter spacecraft (Müller et al., 2013) with the PHI instrument is capable of providing data on the magnetic fields in ARs, but its observations cover only the time interval from 2020 and are not continuous and homogeneous. For the analysis of an earlier time interval, the Solar TErrestrial RElations Observatory (STEREO; Kaiser et al., 2008) spacecrafts are suitable, which also allow one to observe the Sun from other angles, but they do not have instruments for obtaining magnetograms of ARs.

Ultraviolet (UV) radiation is known to be a proxy for the total unsigned magnetic flux: the magnitudes are related by a power-law dependence (Schrijver, 1987). Using data from the STEREO/SECCHI/EUVI instrument, Ugarte-Urra et al. (2015) constructed the continuous graphs of long-term (up to 80 days) variations of UV radiation for some ARs, which can be recalculated into the magnetic flux values.

Visual analysis showed that the UV radiation above unipolar ARs is significantly weakened. In certain cases, in the zone near a sunspot, no UV radiation noticeably pronounced at the background level was observed at all. This fact makes it difficult to use UV radiation to estimate the magnetic flux of such ARs.

The aim of this work is to statistically check for the presence of a deficit of UV radiation in unipolar ARs. It is also of interest to consider whether such a deficit is associated with a low decay rate of the magnetic flux in ARs.

2 Data and methods

To perform this work, we used data from the Helioseismic Magnetic Imager (HMI; Scherrer et al., 2012) and Atmospheric Imaging Assembly (AIA) instruments on board the Solar Dynamics Observatory (SDO; Pesnell et al., 2012). The HMI provides the full-disk maps of the magnetic field vector, radial velocities, and continuum intensity. The AIA records full-disk filtergrams in several lines of the UV range.

The HMI data were used in the form of SHARP CEA, which are the automatically identified patches of ARs with transformation of the Cartesian coordinates into cylindrical (heliographic) coordinates (Bobra et al., 2014). For each AR, we selected patches whose coordinates are no more than 60 degrees away from the central meridian. The interval between patches was six hours.

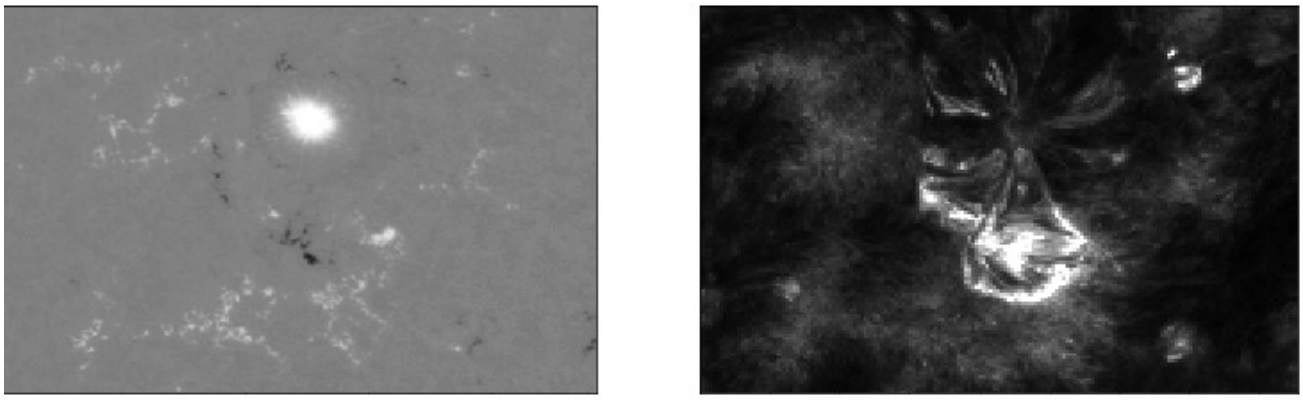

Fig. 1. Magnetogram of the longitudinal magnetic field component (left) and image in the 304 Å line (right) of the NOAA AR 11599 observed on October 31, 2012, at 06:00 UT. The size of the patch in heliographic coordinates is $10.75° \times 14.46°$. It can be seen that the small bipolar element in the lower part of the map generates UV radiation that significantly exceeds the radiation from the large unipolar element in the upper part of the map.

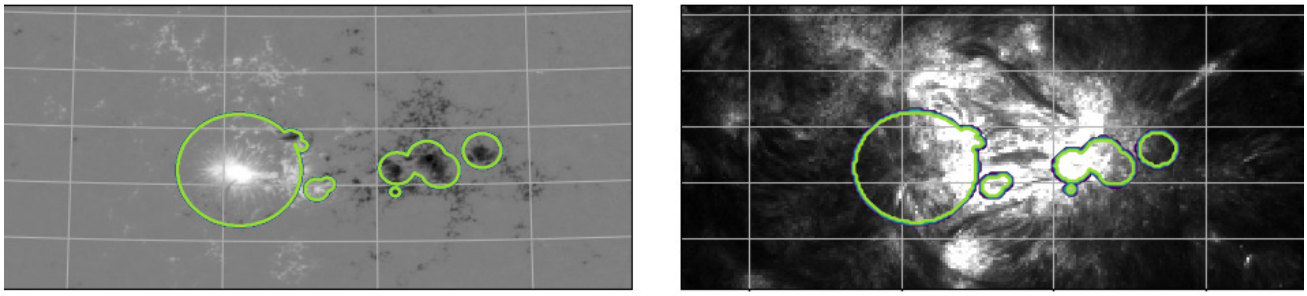

Fig. 2. Magnetogram of the longitudinal magnetic field component (left) and image in the 304 Å line (right) of the NOAA AR 11484 observed on May 20, 2012, at 12:00 UT. The size of the patch in heliographic coordinates is $10.06° \times 20.38°$. The selected mask is shown by the green line.

For each patch, the closest in time AIA map was selected. We used the 304 Å channel corresponding to the He II line formed in the lower part of the transition layer. The AIA image contains a solar full-disk filtergram at a certain wavelength. To compare the HMI and AIA maps, the AIA image was transformed into heliocentric coordinates, then a rectangular section was extracted from it, which corresponds in coordinates to the SHARP CEA patch.

In total, 617 ARs observed from 2010 to 2017 were analyzed, and 87 ARs from the sample were unipolar.

It is worth noting that in some ARs, small bipolar elements can produce UV radiation noticeably exceeding the radiation above sunspots (see an example in Fig. 1). Thus, the total intensity of UV radiation from the entire patch cannot be used as a magnitude corresponding to the UV radiation above the sunspots of an AR since it will significantly depend on the number of emerging elements and, accordingly, on the area of the patch.

In this regard, UV radiation was studied only in the zone of a sunspot and its immediate surrounding for which a mask was used. For all sunspots belonging to the AR, the effective radius was calculated as

$$r_{\text{eff}} = \sqrt{\frac{S}{\pi}},$$

where S is the area of a sunspot in pixels calculated as the area inside the isoline with the white light radiation below 0.65 of the quiet Sun intensity. In other words, r_{eff} is the radius of a circle equal in area to a sunspot. The mask was defined as a circle with a radius of $5r_{\text{eff}}$ with a center in the pixel belonging to the sunspot with the lowest white light intensity. The final mask was defined as a disjunction (union) of all masks of sunspots belonging to the AR. An example of the mask selection is shown in Fig. 2.

The value of the magnetic flux was calculated as

$$\Phi = \sum_{P} |B_r \Delta S|,$$

where B_r is the radial component of the magnetic field in a pixel, ΔS is the area element corresponding to the pixel, and P are the pixels belonging to the patch. To reduce the influence of instrument artifacts, only B_r values exceeding 600 Mx cm^{-1} in modulus were summed (Norton et al., 2017). (It should be noted that in Norton et al. (2017), a threshold of 575 Mx cm^{-1} was used.)

The radiation intensity was calculated as

$$I = \sum_{M} I_{\text{AIA}},$$

where I_{AIA} is the radiation intensity in the pixel of the AIA map after recalculation into cylindrical coordinates, and M are the pixels belonging to the mask.

Since the area covered by the mask explicitly depends on the area of sunspots and can consequently vary, it is appropriate to introduce the UV radiation density (intensity per unit area):

$$i = \frac{I}{N_M},$$

where N_M is the number of pixels in the mask. Thus, for each AR we obtain three time-dependent series of quantities: $\Phi(t), I(t), i(t)$.

The processing program was written in the Python programming language using the Astropy (Astropy Collaboration et al., 2022), Sunpy (The SunPy Community et al., 2020), Numpy (Harris et al., 2020), and Scipy (Virtanen et al., 2020) libraries. Images were generated using the Matplotlib library (Hunter, 2007).

3 Results

Figure 3 shows a scatter plot between the UV radiation density i and the total unsigned magnetic flux Φ in ARs. One point on the graph corresponds to one pair of maps of UV radiation and magnetic field. Observations belonging to unipolar ARs are marked in orange, and the ARs of other classes are in blue. It can be seen from the graph that the distributions differ noticeably: while for unipolar ARs the UV radiation density increases with increasing magnetic flux of an AR (the correlation coefficient between the logarithms of the values is 0.49), for ARs of other classes this value practically does not depend on the magnetic flux of an AR (the correlation coefficient between the logarithms of the values is 0.11). Meanwhile, the cloud of points corresponding to unipolar ARs is located lower on the graph than the points belonging to the ARs of other classes.

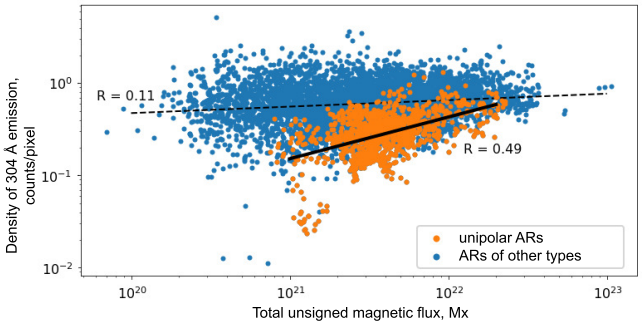

Fig. 3. Scatter plot between the UV radiation density and the total unsigned magnetic flux of ARs. One point corresponds to one magnetogram. Unipolar ARs are shown in orange, and ARs of other classes are in blue. The approximation between the values for unipolar ARs is indicated by the solid black line, and for ARs of other classes by the dashed line.

The average radiation density for unipolar ARs is 0.32 counts per pixel, while for ARs of other classes it is 0.68 counts per pixel. The mean square deviations for the sets are 0.16 and 0.35 counts per pixel, respectively. The Kolmogorov–Smirnov test also confirms the assumption that these quantities have different distributions: the statistic of D is 0.58, and it significantly exceeds the critical value 0.05.

When expressing i in counts per pixel, Φ in Mx, and substituting numerical values, the approximation between the values of UV radiation density and magnetic flux for unipolar ARs has the form

$$i = 2.53 \cdot 10^{-11} \Phi^{0.46}. \quad (1)$$

To compare the radiation density with the magnetic flux decay rate, the value of <i> was calculated, which is the averaging in time for the series of $i(t)$. The magnetic flux decay rates for various ARs are taken from Plotnikov et al. (2023).

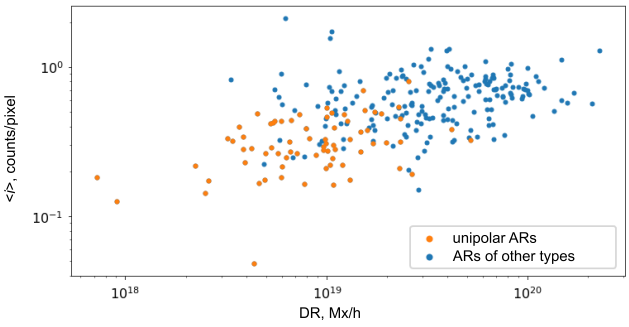

Fig. 4. Scatter plot between the average UV radiation density and the magnetic flux decay rate. One point corresponds to one AR. Unipolar ARs are shown in orange, and the ARs of other classes are in blue.

Figure 4 shows a scatter plot between <i> and the decay rate DR. One point on the graph corresponds to one AR. Since the samples in this work and in Plotnikov et al. (2023) do not coincide, only 258 ARs studied in both works are included in the graph. As in Fig. 3, unipolar ARs are indicated in orange, and ARs of other classes are in blue. The correlation coefficient between the logarithms of the values is 0.54. The presence of a correlation does not contradict the previous conclusion that the UV radiation density in bipolar and multipolar ARs varies weakly. Indeed, if we divide these samples by classes, it turns out that for unipolar ARs the correlation coefficient between the logarithms of UV radiation density and magnetic flux decay rate will be 0.41, and for ARs of other classes 0.23. That is, for ARs of other classes, the UV radiation density above sunspots also varies weakly with changes in the magnetic flux decay rate (which is related by a power-law dependence to the peak magnetic flux in an AR). The presence of a correlation for the entire sample is largely due to the fact that unipolar ARs have on average both lower UV radiation density and lower decay rate.

4 Conclusions and discussion

Based on a sample of 617 ARs of various magnetomorphological classes, the following patterns were found:

- The UV radiation density in the 304 Å channel above sunspots for unipolar ARs is on average lower than for ARs of other classes. The average intensity density values for these subsets are 0.32 ± 0.16 and 0.68 ± 0.35 counts/pixel, respectively.
- For bipolar and multipolar ARs, the UV radiation density above sunspots weakly depends on the total unsigned magnetic flux of an AR.
- For unipolar ARs, the dependence between the UV radiation density above sunspots and the total unsigned magnetic flux can be expressed as $i = 2.53 \cdot 10^{-11}\Phi^{0.46}$, where i is expressed in counts per pixel, while Φ is normalized by 1 Mx to have unitless quantity under the exponent.
- The UV radiation density above sunspots weakly varies with the magnetic flux decay rate for ARs of all classes. However, the presence of a correlation between these values for the entire sample is largely due to the fact that unipolar ARs have on average both lower UV radiation density and lower decay rate.

For 258 ARs also studied in Plotnikov et al. (2023), it was found that the magnetic flux decay rate in ARs correlates with the UV emission density above sunspots.

The UV emission density above sunspots in unipolar ARs is on average lower than in ARs of other classes and depends on the magnetic flux of an AR. Therefore, even if the relationship from Schrijver (1987) (a power-law dependence between the UV emission generated by an AR and its total unsigned magnetic flux) holds for unipolar ARs, then the coefficients of the relationship will differ from those for ARs of other classes. This complicates the use of this dependence for estimating the magnetic flux of unipolar ARs behind the limb. However, the dependence from equation (3) can be used instead of estimating the magnetic flux of such ARs.

The reason for the reduced UV emission density above sunspots in unipolar ARs may be the more vertical orientation of magnetic field lines (relative to the surface). In such a configuration, a smaller portion of the magnetic flux tube will lie in the region of formation of the 304 Å spectral line compared to bipolar ARs (where magnetic loops lie closer to the solar surface and thus have a greater inclination relative to the normal). Along with the explicit dependence between UV emission density and magnetic flux decay rate, this fact may shed light on the reasons for the slow flux loss in some unipolar ARs.

Acknowledgments. The author is grateful to the referee for constructive comments that helped to improve the paper. The work was supported by the state assignment No. 122022400224-7.

References

Astropy Collaboration, Price-Whelan A.M., Lim P.L., et al., 2022. Astrophys. J., vol. 935, no. 2, p. 167.
Bobra M.G., Sun X., Hoeksema J.T., et al., 2014. Solar. Phys., vol. 289, no. 9, pp. 3549–3578.
Harris C.R., Millman K.J., van der Walt S.J., et al., 2020. Nature, vol. 585, no. 7825, pp. 357–362.
Hunter J.D., 2007. Comput. Sci. Eng., vol. 9, no. 3, pp. 90–95.
Kaiser M.L., Kucera T.A., Davila J.M., et al., 2008. Space Sci. Rev., vol. 136, no. 1–4, pp. 5–16.
Müller D., Marsden R.G., St. Cyr O.C., Gilbert H.R., Solar Orbiter Team, 2013. Solar. Phys., vol. 285, no. 1–2, pp. 25–70.
Norton A.A., Jones E.H., Linton M.G., Leake J.E., 2017. Astrophys. J., vol. 842, no. 1, p. 3.
Pesnell W.D., Thompson B.J., Chamberlin P.C., 2012. Solar. Phys., vol. 275, no. 1–2, pp. 3–15.
Plotnikov A.A., Abramenko V.I., Kutsenko A.S., 2023. Mon. Not. Roy. Astron. Soc., vol. 521, no. 2, pp. 2187–2195.
Scherrer P.H., Schou J., Bush R.I., et al., 2012. Solar. Phys., vol. 275, no. 1–2, pp. 207–227.
Schrijver C.J., 1987. Astron. Astrophys., vol. 180, no. 1–2, pp. 241–252.
The SunPy Community, Barnes W.T., Bobra M.G., et al., 2020. Astrophys. J., vol. 890, p. 68.
Ugarte-Urra I., Upton L., Warren H.P., Hathaway D.H., 2015. Astrophys. J., vol. 815, no. 2, p. 90.
Virtanen P., Gommers R., Oliphant T.E., et al., 2020. Nature Methods, vol. 17, pp. 261–272.